Appl. Statist. (1995)
44, *No.* 1, *pp.* 17–30

A Functional Data Analysis of the Pinch Force of Human Fingers

By J. O. RAMSAY† and X. WANG

McGill University, Montreal, Canada

and R. FLANAGAN

University of Cambridge, UK

[Received May 1993. Final revision March 1994]

SUMMARY

The ability of the human thumb and forefinger to adapt the pinch force to the static and dynamic characteristics of the object being grasped is one of the marvels of human physiology. We analyse a sample of records of the force applied during a brief squeeze by functional data analysis techniques in which familiar statistical concepts are adapted to observations that are functional in character. Except for scale, a graph of these force impulses closely resembles a log-normal density function, and this has a plausible physiological rationale. Specially adapted smoothing spline approximations along with a functional version of principal components analysis reveal that the residual variation is essentially one dimensional in structure, and that the force functions can be described by a simple linear differential equation incorporating the effects of drag or viscosity in the joints and muscles involved.

Keywords: Differential equation; Functional data analysis; Log-normal distribution; Motor control; Spline smoothing

1. Introduction

One of the most remarkable muscle groups in the human body controls the thumb and forefinger in the act of gripping an object. The force exerted must be adapted to the object's weight, acceleration, surface texture, contour and structure. Moreover, the system is slow relative to the response speeds that are often required by the external world; a best response time of the order of 100 ms must cope with event sequences such as occur in typing or piano playing that often are of the order of 10 ms or less, implying that the brain must often anticipate the required force. Understanding this system better can yield insights into how the brain can control high performance motor systems such as the hand and the tongue in the context of rapidly changing task characteristics. This knowledge may also lead to better robot design.

The data discussed in this paper were collected at the Medical Research Council Applied Psychology Unit, Cambridge, by the third author as a part of a sequence

†*Address for correspondence*: Department of Psychology, McGill University, 1205 Dr Penfield Avenue, Montréal, Québec, H3A 1B1, Canada.
E-mail: ramsay@psych.mcgill.ca

 0035–9254/95/44017

of experiments and consist of records of the force exerted by pinching a force meter (width 6 cm) with the tips of the thumb and forefinger on opposite sides. The task required of the subject was

(a) to maintain to within reasonable limits a constant force determined by the experimenter,
(b) on a signal to give a brief force impulse which was targeted to reach a predetermined maximum value and
(c) to return the force to the constant background level.

The constant background force, the targeted maximum force and the subjects were all varied in the results discussed here. Within a fixed set of conditions, as many as 100 replications were obtained.

Fig. 1 shows 20 typical records in which the background force and the maximum force were 2 N and 10 N respectively. Although there is considerable variation from replication to replication in aspects of these functions, we naturally expect that certain characteristics of the shape will remain quite stable. Fig. 1 indicates that records vary substantially in terms of time of the maximal force, the size of this force and its duration, but that each record closely maintains a common basic shape.

These are an example of functional data, meaning that the basic or primitive observation is a function, here force as a function of time. In this paper we apply the techniques of functional data analysis as described by Ramsay and Dalzell (1991) to uncover the processes that determine the typical record as well as the variation between records. Our objective is the representation of this process by a simple differential equation which appears to be consistent with the known physiology of the system.

In the following section we develop the model that will motivate and define the subsequent analyses. This model leads to the development and application of a spline smoothing process which is adapted to the characteristics of the model and

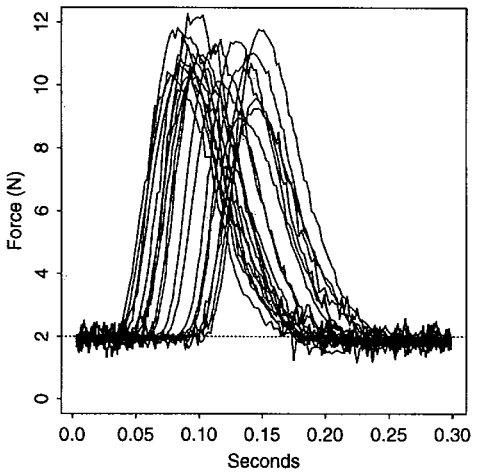

Fig. 1. 20 recordings of the force exerted by the thumb and forefinger where a constant background force of 2 N was maintained before a brief impulse targeted to reach 10 N: the force was sampled 2000 times per second

data. Section 4 shows that applying a functional version of principal components analysis reveals the variation between force records to be essentially unidimensional. The next section discusses these findings in terms of motor control physiology. Technical matters are relegated to Appendix A.

2. Log-normal Model for Pinch Force

If we subtract the background force, the shape of the records in Fig. 1 resembles that of various familiar probability density functions, except that the area under the curve is not normalized. The positive skewness in the records tends to be about what we find in the log-normal density, which is usually expressed as

$$p(t) = (2\pi)^{-1/2} t^{-1} \exp\left\{ -\frac{(\ln t - \ln \mu)^2}{2\sigma^2} \right\},$$

where μ and σ are location and scale parameters respectively, For our purposes, the following less familiar but equivalent form is more useful because it eliminates the factor t^{-1}:

$$p(t) = (2\pi)^{-1/2} \exp\left(-\ln \mu + \frac{\sigma^2}{2} \right) \exp\left[-\frac{\{\ln t - (\ln \mu - \sigma^2)\}^2}{2\sigma^2} \right]. \tag{1}$$

Expressed in this way, it is more obvious that the maximum of this function, or the modal value, is $t = \ln \mu - \sigma^2$. This formulation suggests the model

$$f(t) - f_0 = C \exp\left[-\frac{\{\ln(t - t_0) - \ln(t_M - t_0)\}^2}{2\sigma^2} \right], \qquad t > t_0, \tag{2}$$

where $f(t)$ is the force exerted at time t, f_0 is the targeted background force, C is the maximum force, t_0 is the time of origin of the force impulse, t_M is the time of the maximum force and σ is a shape parameter.

To simplify the notation, we shall henceforward assume that force is measured relative to the targeted background force as origin, and thus that we are interested in the part of the force impulse that exceeds f_0, i.e. we shall assume that $f_0 = 0$.

This model has a motivation that is interesting both substantively and statistically. If we imagine that the response of a muscle system at time t is proportional to the rate of arrival of discrete events such as neural impulses arriving on many independent channels, such as separate nerve fibres, and if it is supposed that the disturbance processes which cause these events to have a random distribution are sequential and multiplicative in character, then the central limit theorem implies convergence to a response function of this nature. Plamondon (1992) proposed this process to explain the shape of velocity curves for very rapid hand movements during handwriting, where a closely similar pattern is observed. Alternative explanations are taken up in Section 5.

Clearly the four parameters C, t_0, t_M and σ must be estimated separately for each curve. Expressing model (2) in the equivalent form

$$\ln f(t) = -b_0 - b_1 \ln(t - t_0) - b_2 \{\ln(t - t_0)\}^2, \tag{3}$$

we note that conditional on t_0 the other parameters can be estimated by least squares. We used only force values that exceeded the background force f_0 by 0.5 N

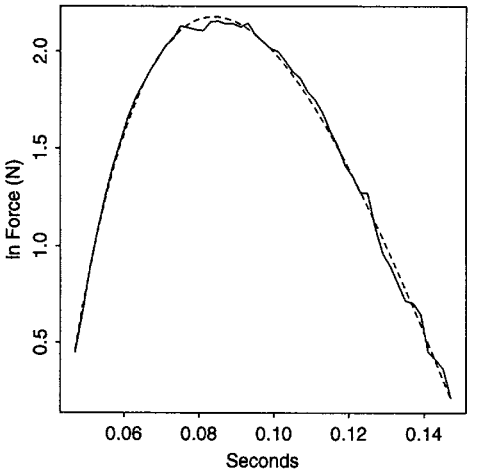

Fig. 2. Single log-force record for forces exceeding 2.5 N: -----, fit by least squares of model (3), which is quadratic in log-time

and employed a simple grid search technique to identify the least squares estimate of t_0. Fig. 2 displays a typical single record for the logarithm of the amount that the pinch force exceeded the threshold, along with the fit by least squares. This simple model accounted for about 97% of the variation within each record.

The quadratic approximation to log-suprathreshold force can also be used to define a common origin and scale. The linear transformation of time

$$s = \frac{t - t_0}{t_M - t_0}, \tag{4}$$

where t_M is the time of maximum force, implies that log-suprathreshold force as a function of $\ln s$ is symmetric about $s = 1$, and hence that the model simplifies to

$$\ln f(s) = -b_0^* - b_2^* (\ln s)^2$$

and

$$f(s) = \exp\{-b_0^* - b_2^* (\ln s)^2\} = C \exp\{-(\ln s)^2/2\sigma^2\}, \tag{5}$$

where $C = \exp(-b_0^*)$ and $\sigma^2 = (2b_2^*)^{-1}$.

The integral of the force curve

$$E = (t_M - t_0) \int_0^\infty f(s)\, ds$$

$$= (t_M - t_0)\sqrt{(2\pi)} C\sigma \exp(\sigma^2/2) \tag{6}$$

is a useful descriptor of the total response effort. The time to maximum force $t_M - t_0$, maximal force C and the shape-dependent function $\sigma \exp(\sigma^2/2)$ combine multiplicatively to define this measure, at least as far as model (2) is concerned.

If the variation of spread parameter σ^2 over replications is a nuisance, we can further normalize the force function by working with

$$f^*(s) = C\{f(s)/C\}^{\sigma/\sigma_0} \tag{7}$$

which has the fixed spread parameter σ_0^2.

Table 1 shows the characteristics of the main descriptors of the 20 curves in Fig. 1, time to maximum force $t_M - t_0$, maximum force C, spread σ and effort E. The coefficients of variation for both maximal force and effort E are especially small. Table 2 indicates the corresponding correlations between these descriptors. We see that there is a very strong negative correlation between time to maximum force and spread, so that their net contribution to effort tends to be fairly stable. Consequently, effort is primarily related to maximum force, suggesting perhaps that the system is designed to expend energy principally to reach a target force maximum, as opposed to controlling the shape of the force impulse.

Model (5) can also be expressed as a differential equation:

$$\frac{df}{ds} = -\frac{1}{\sigma^2}\frac{\ln s}{s} f(s). \tag{8}$$

From this we can see that $-1/\sigma^2$ is the slope in the linear relationship between f' and $(f \ln s)/s$, and therefore that σ^2 is the slope of the normal to this line. Fig. 3 plots the relationship between the first difference of force and the right-hand side $(f \ln s)/s$ for a typical force impulse.

Associated with this differential equation is the linear differential operator

$$(Lf)(s) = \frac{1}{\sigma^2}\frac{\ln s}{s} f(s) + \frac{df}{ds} \tag{9}$$

or

$$L = \frac{1}{\sigma^2}\frac{\ln s}{s} I + D.$$

TABLE 1
Summary statistics for 20 pinch force function descriptors (after subtracting the base-line force)

Statistic	$t_M - t_0$	C	σ	E
Mean	0.084	8.96	0.286	0.549
Standard deviation	0.017	0.857	0.045	0.059
Coefficient of variation	0.197	0.096	0.157	0.107

TABLE 2
Correlations between the pinch force function descriptors

	$t_M - t_0$	C	σ	E
$t_M - t_0$	1.00	−0.31	−0.97	−0.24
C	−0.31	1.00	0.34	0.95
σ	−0.97	0.34	1.00	0.32
E	−0.24	0.95	0.32	1.00

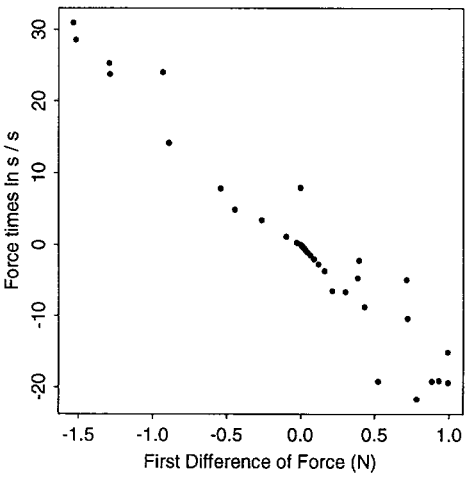

Fig. 3. Relationship between the right-hand side of equation (8) and the first difference of force for a typical single record: its strong linearity indicates that the differential equation (8) describes well this force impulse

This operator satisfies the homogeneous equation $Lf = 0$ when f is a member of family (5).

This differential equation formulation is critical to the functional data analyses to be developed and displayed here. The description of the model in terms of a differential equation can also be motivated by considering that a large proportion of the important functional relationships in the natural sciences are most meaningfully expressed as simple differential equations, and we can therefore hope that these data may also display a simple structure when expressed in these terms. Moreover, in exploring departures from the basic log-normal model, it will turn out to be revealing to identify the non-homogeneous differential equation

$$Lf = u. \tag{10}$$

Function u is often called the *forcing function* and tends in applications to describe the effects of external factors on the system.

3. Smoothing Data to Identify Residual Variation

It would be naïve to suppose that the log-normal model (2) or (5) is completely adequate to describe force impulses. Our goal in this section is to fit nonparametrically a record (s_i, y_i), $i = 1, \ldots, n$, where y_i is the observed force at sampling point i at transformed time s_i, by the more general smoothing function

$$h(s) = f(s) + e(s).$$

The first term f is the model component (5) and the second term e is the additional signal or residual function that is necessary to give an adequate account of the actual data. But we can identify term e uniquely only if it satisfies some suitable constraint that separates its contribution from that potentially provided by term f. There are many ways to do this, but a natural approach here would be to constrain the residual function e to contribute zero to the total effort E. Thus, we specify that

$$\int_0^\infty e(s)\,ds = 0.$$

For technical reasons mentioned in Appendix A, this must be modified to

$$\int_{S_0}^{S_1} e(s)\,ds = 0. \tag{11}$$

The limits of integration here must contain the observed values of the transformed times s_i and must also satisfy $0 < S_0 < S_1 < \infty$. We can always choose these limits so that this is a reasonable approximation to the constraint, and therefore so that the residual function $e(s)$ in effect contributes negligibly to the effort E.

Individual records in Fig. 1 show clearly that there is some fairly small amount of noise or error variation in the observations that would not be reasonable to fit by h, possibly because of aspects of the recording process. This suggests the use of the smoothing spline criterion

$$Q = \sum_{i=1}^{n} \{y_i - h(s_i)\}^2 + \lambda \int (Lh)^2(s)\,ds. \tag{12}$$

The first term is a least squares error term, and the second term measures the departure from smoothness in terms of the size of the function $Lh = L(f + e) = Le$, where L is the differential operator (9). We can motivate the choice of the second term by asking that as much of the variation in the data as possible be accommodated by the model term f since we are interested only in residual influences e that absolutely cannot be accounted for by the model. We penalize the size of Le because we shall be interested in the description of residual term e in terms of the differential equation $Le = u$, and it is reasonable from this perspective to ask that the forcing function u be small.

The smoothing parameter λ controls the penalty to be placed on $\|Lh\|^2$. A very large value implies that virtually all the fit is to be achieved by the model term f, and as λ goes to 0 the observations will be interpolated rather than smoothed.

Appendix A gives the technical details of the computation of the smoothing function h_j for record j. We used the power transformation (7) to standardize the spread of the force impulses to the value $\sigma = 0.05$. The limits of integration in equation (11) were 0.4 and 2.4, and these included all the observed values of s_i. As the number of sampling points varied from record to record, we used linear interpolation to estimate suprathreshold force impulse values at the common set of 41 sampling points from $s = 0.4$ to $s = 2.4$ in steps of 0.05. But where these common sampling points fell outside the range of observed sampling points for a particular record we used the values of the fitted model (5). We used the data-driven generalized cross-validation technique described by Wahba (1990) to choose an appropriate value for the smoothing parameter λ, which turned out to be about 1. Rice and Silverman (1991) proposed an alternative technique for smoothing parameter identification, and still other methods are reviewed in Green and Silverman (1994).

Fig. 4 shows the fitted function h for a typical record as a full curve, along with the model component f as a broken curve. We see here, as in Fig. 2, that the actual force impulse is a little flatter at its maximum than model (5) allows for, and that

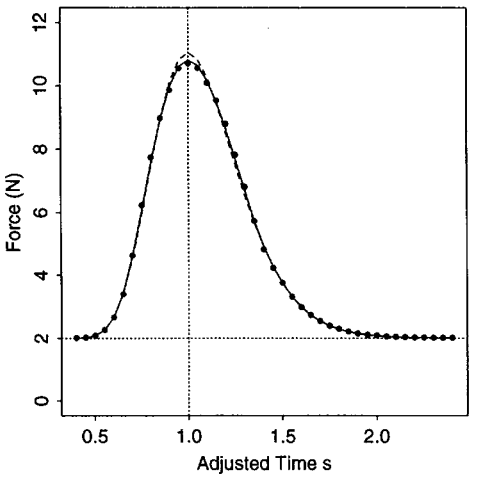

Fig. 4. Smoothing spline fit h (———) to a typical record: •, observed suprathreshold forces; -----, log-normal model component f

it falls off a trifle more slowly after the maximum. The largest discrepancy between h and f is only about 2% of the peak force, however.

The average residual function $\bar{e}$ for a set of 20 force impulses where the target was 10 N and the base-line force was 2 N is shown in Fig. 5. The function has an integral which is near 0, and the negative lobe at $s = 1$ accommodates the fact that h is flatter at the point of maximal force than model f. The largest modulus of the mean $\bar{e}$ is only about 3% of the target force.

4. Principal Components of Variation in Force Impulses

The force impulses can potentially vary from record to record in a great variety

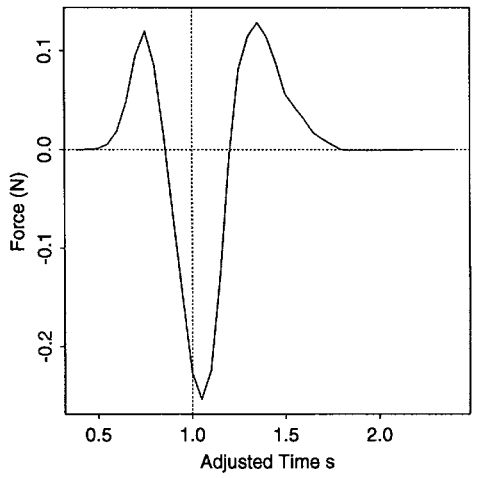

Fig. 5. Average residual function $\bar{e}$ for a set of 20 force impulses where the target force was 10 N and the base-line force was 2 N

of ways. By the transformation to time measure s we have eliminated a variation in origin and timing of the maximum, and by standardizing the spread parameter σ to 0.05 we have effectively constrained the area under the curves to be proportional to the maximum force C. But a large range of potential variation remains.

Variation from record to record in the model component f is essentially one dimensional, and one approach to studying this variation would be simply to display the variability in the coefficient C in model (2).

Exploring the variation in the residual functions e is both more interesting and more challenging, however, since these can potentially vary in shape in complex ways. Ramsay (1982), Besse and Ramsay (1986) and Ramsay and Dalzell (1991) developed a version of principal components analysis for functional data which was designed to ascertain how many modalities of variation are to be found among a set of replicated functions. In one version of their approach, only variation in the residual function e is taken into account. This involves the spectral analysis of the bivariate variance-covariance function

$$v(s, t) = N^{-1} \sum_{j}^{N} e_j(s)\, e_j(t). \tag{13}$$

The motivation for the choice of fitting criterion (12) was that the transformed functions Le might be of interest, and that their variation in size should be controlled in fitting the data. Following this approach, it would seem that it is the variability in Le that should be explored, and that the functional principal components analysis should be applied at this level rather than to e and v directly. Consequently, it is the eigenequation

$$\int_{S_0}^{S_1} \{L\, v(s, \,)\}(w)(L\xi)(w)\, \mathrm{d}w = \mu\, \xi(s) \tag{14}$$

that is solved for eigenvalue μ and eigenfunction ξ in this version of functional principal components analysis. Any two eigenfunctions are required to satisfy the orthonormality constraint

$$\int_{S_0}^{S_1} (L\xi_j)(s)(L\xi_k)(s)\, \mathrm{d}s = \delta_{jk}, \tag{15}$$

where $\delta_{jk} = 1$ if $j = k$ and $\delta_{jk} = 0$ otherwise. The size of an eigenvalue μ indicates the contribution of the associated eigenfunction to the variation between the residual functions e_j. In effect, then, equation (14) describes the principal components analysis of the forcing functions. Further technical details concerning this analysis are provided in Appendix A.

For the data that yielded Fig. 5, there was only one substantial eigenvalue, and this accounted for 76% of the variation. In the principal components analysis of non-centred data where there is only one strong component of variation, this will closely resemble the mean function. Consequently, the first eigenfunction for these data looks very much like the mean function $\bar{e}$ displayed in Fig. 5.

Because the orthogonality constraints on the eigenfunctions are defined in terms of $L\xi$, it is more natural to examine the result of applying differential operator L to an eigenfunction than it is to view the eigenfunction directly. Fig. 6 shows the first function $L\xi$. In the neighbourhood of $s = 1$, $L\xi$ has the shape of a step

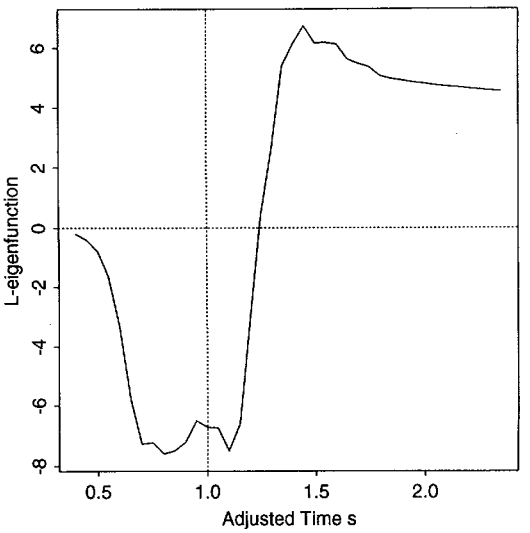

Fig. 6. Result of applying differential operator L to the first eigenfunction of the variance–covariance function for the force impulse data

function, with a negative phase swinging abruptly to a positive phase at around time $s = 1.2$. Its behaviour for more extreme values of s is less interesting because it is a consequence of the spline smoothing process that this function must be 0 at the extremes.

A second and less important eigenfunction appears for some experiments. For the data analysed in this paper, this eigenfunction contributes only to one curve, and it primarily captures a slight misalignment between the model component and the observed force impulse, and is due to the failure of the preliminary quadratic fitting process to locate properly the time to peak force. That is, errors in the estimation of t_0 and t_M result in values of transformed time s which are slightly off.

The stability of these findings across various values of the base-line and targeted forces, and across subjects, was remarkable. The general features observed in Figs 5 and 6 remain essentially unchanged except for variation in amplitude.

5. Discussion and Conclusion

It seems that the pinch force system can be described to an impressive level of accuracy by the differential equation

$$\frac{\mathrm{d}f}{\mathrm{d}s} + \frac{1}{\sigma^2}\frac{\ln s}{s} f(s) = u(s),$$

where

$$u(s) = \begin{cases} U_1 < 0 & s \leqslant 1.2, \\ U_2 > 0 & s \geqslant 1.2 \end{cases} \tag{16}$$

and $s = (t - t_0)/(t_M - t_0)$.

We hypothesize that the forcing function u is due primarily to drag or viscosity

in the motor system. This would explain why the peak of the force impulse does not rise as high as the model would predict, since drag would retard the build-up of force. As the muscles relax following maximum force, we would expect that drag would exert the opposite effect, retarding the decline in force and the slight physical movement in the thumb and forefinger.

Just why the log-normal function defined by $Lf = 0$ should provide such an excellent first approximation to the data is a fascinating question. Crow and Shimizu (1988) reviewed the many applications of the log-normal distribution in applied statistics. Ulrich and Miller (1993) considered specific mathematical models that might generate log-normal reaction times.

The supposition that the logarithm of the process is a result of independent or nearly independent increments tends to motivate many of these discussions. Plamondon (1991, 1992) argued along these lines for velocity functions during rapid hand movements such as we might encounter, for example, in handwriting.

However, the log-normal function could arise from something nearly like an exponential transformation superimposed on a normally distributed process, with the latter possibly due to central limit effects. Feldman (1986) suggested that force depends exponentially on muscle activation.

Although this paper is aimed primarily at statisticians who are interested in applying functional data analysis to these and other problems, we offer some remarks about motor physiology, of which there is a recent review by Rothwell (1987). The pinch response is the result of the activity of very many motor units (MUs), each consisting of a motoneurone axon, terminal branches and the muscle fibres that it innervates. There are about 100 fibres per MU in hand muscles, and each fibre is activated by only a single parent motoneurone. When an MU is activated, waves of depolarization called action potentials travel down the motoneurone branches and activate all the associated fibres in synchrony. Thus the MU represents the smallest number of fibres that can be activated by the central nervous system.

Ultimately, because many different hand muscles will contribute to the generation of brief force pulses, hundreds if not thousands of MUs may be activated, each of which is associated with of the order of 100 individual muscle fibres. In these circumstances, it seems reasonable to propose that the total force exerted is the result of the rate of arrival of relatively independent events, these being the action potentials activating individual fibres. If we accept this, then the data indicate that the stochastic nature of the arrival times closely resembles that of the log-normal distribution.

However, this simple explanation ignores many complexities at the level of individual MUs, and there are many references on the individual behaviour of MUs. Ulrich and Wing (1991) developed a recruitment model at this level based on the Erlangian or gamma distribution. Moreover, the build-up of force also depends on the length of time that an individual muscle fibre takes to develop maximum force once stimulated, as well as on the variability in stimulation times.

At best we can say that the measured pinch force is the result of a cascade of complex processes, the end result of which is something remarkably like a log-normal response function, modulated only slightly by what appears to be drag or viscosity. We wonder, along with Plamondon (1991, 1992), just how many short-lived motor events display this effect.

The analyses reported in this paper are not the only ones possible which are likely to reach the same conclusions. Ansley *et al.* (1993) have also developed an approach to nonparametric regression incorporating prior information through the use of linear differential operators. The first author of the present paper has developed a discretized approach using divided differences instead of derivatives that comes very close to reproducing these results, but which is substantially simpler to implement. The principal components analysis results can also be achieved in other ways, and the method of Rice and Silverman (1991) that penalizes the roughness of eigenfunctions is an effective alternative approach.

It strikes us as exciting that the techniques of functional data analysis have revealed this simple two-dimensional structure in these data, and that this structure can be so neatly captured by the simple differential equation $Lf = u$. An essential step in the functional data analysis carried out here was to tailor the smoothing process to the known structure of the data. This is done by first identifying a model or simple function which accounts for a large portion of the variation in the observations, and which has some substantive significance. By designing the spline smoother around this model, we can study the behaviour of the remaining variation via principal components analysis and thus identify the additional influences or forcing functions which also play a significant role. We believe that functional data analysis carried out along these lines has an exciting future.

Acknowledgements

The research reported in this paper was supported by grant APA0320 from the Natural Sciences and Engineering Research Council of Canada to J. O. Ramsay. The data were collected by R. Flanagan during his tenure as a Natural Sciences and Engineering Research Council Postdoctoral Fellow at the Medical Research Council Applied Psychology Unit at Cambridge, and analysed by Xiaohui Wang as a part of her graduate studies at McGill University.

Appendix A

It is a standard result in the theory of spline functions (Wahba, 1990) that the solution h to the spline smoothing problem (12) can be expressed in the form

$$h(s) = \sum_{i=1}^{m} d_i f_i(s) + \sum_{j=1}^{n} c_j k(s_j, s)$$

where the functions f_i span the space of functions satisfying $Lf = 0$, and where the bivariate function k is the reproducing kernel for the Hilbert space of functions e satisfying $\int e = 0$ and with the inner product

$$(e_j, e_k) = \int (Le_j)(s)(Le_k)(s)\,\mathrm{d}s.$$

In this application there is only a single function f associated with the kernel of the operator L, and the main technical issue is the computation of k. The reproducing kernel has a simple relationship to the Green function $g(s; w)$ satisfying the equation

$$e(s) = \int_{S_0}^{S_1} g(s; w)(Le)(w)\,\mathrm{d}w, \tag{17}$$

namely

$$k(s, t) = \int_{S_0}^{S_1} g(s;\ w)\, g(t; w)\, \mathrm{d}w.$$

The Green function in effect defines an integral transform which is the inverse of the differential operator L, and $g(s; w)$ plays a key role in all aspects of the theory of functions associated with this situation. Therefore the most basic problem is to specify this Green function.

Dalzell and Ramsay (1993) developed a method for computing the Green function associated with constraint (11) and differential operator L. The Green function for this problem is

$$\begin{aligned} g(s; w) &= F(w) \exp\left\{\frac{(\ln w)^2 - (\ln s)^2}{2\sigma^2}\right\}, \qquad S_0 \leqslant w < s, \\ g(s; w) &= \{F(w) - 1\} \exp\left\{\frac{(\ln w)^2 - (\ln s)^2}{2\sigma^2}\right\}, \qquad S_1 \geqslant w \geqslant s, \end{aligned} \tag{18}$$

where

$$F(w) = \frac{\int_{S_0}^{w} \exp\{(\ln u)^2/2\sigma^2\}\, \mathrm{d}u}{\int_{S_0}^{S_1} \exp\{(\ln u)^2/2\sigma^2\}\, \mathrm{d}u}.$$

It turns out that we can express $F(w)$ as

$$F(w) = \frac{\Phi(\sigma^{-1} \ln w - \sigma) - \Phi(\sigma^{-1} \ln S_0 - \sigma)}{\Phi(\sigma^{-1} \ln S_1 - \sigma) - \Phi(\sigma^{-1} \ln S_0 - \sigma)}$$

where Φ is the standard normal distribution function, for which approximations are well known. It is apparent that for practical computation we must have $S_0 > 0$ and $S_1 < \infty$. The integration required to compute values of the reproducing kernel k from the Green function must be performed numerically, but $g(s; w)$ is a smooth function of w on either side of s, and we found that quadrature using Romberg extrapolation (Stoer and Bulirsch, 1980) was quite satisfactory.

Let vector $\mathbf{f}$ contain the values $f(s_j)$, $\mathbf{y}$ contain y_j and matrix $\mathbf{K}$ contain the values $k(s_i, s_j)$, $i, j = 1, \ldots, n$. Then the coefficient d and coefficient vector $\mathbf{c}$ defining the smoothing spline h satisfy the linear equations

$$\mathbf{Mc} + \mathbf{f}d = \mathbf{y},$$

$$\mathbf{f}'\mathbf{c} = 0$$

from which we have

$$d = \mathbf{f}'\mathbf{M}^{-1}\mathbf{y}/\mathbf{f}'\mathbf{M}^{-1}\mathbf{f}$$

and

$$\mathbf{c} = \mathbf{M}^{-1}(\mathbf{y} - \mathbf{f}d)$$

where $\mathbf{M} = \mathbf{K} + n\lambda\mathbf{I}$. For large n and/or closely spaced values of s_i, the matrix $\mathbf{M}$ can be very ill conditioned, and Wahba (1990) should be consulted for further computational details.

Besse and Ramsay (1986) and Ramsay and Dalzell (1991) showed that the principal components analysis implied by eigenequation (14) can be expressed in matrix terms as follows. Let $\mathbf{E}$ be the 20×41 matrix of values of $e_j(t_i)$, where j indexes records. The corresponding variance-covariance matrix is $\mathbf{V} = N^{-1}\mathbf{E}'\mathbf{E}$, where $N = 20$ is the number of functions. Let the order 41 positive semidefinite matrix $\mathbf{N}$ be defined as

$$\mathbf{N} = \{\mathbf{f}(\mathbf{f}'\mathbf{f})^{-1}\mathbf{f}' + \mathbf{K}\}^{-1}\mathbf{K}\{\mathbf{f}(\mathbf{f}'\mathbf{f})^{-1}\mathbf{f}' + \mathbf{K}\}^{-1}. \tag{19}$$

Then a matrix eigenequation that is equivalent to equation (14) is

$$\mathbf{VNu} = \mu\mathbf{u} \tag{20}$$

where the eigenvector $\mathbf{u}$ is subject to the normalization $\mathbf{u}'\mathbf{Nu} = 1$. In effect, matrix $\mathbf{N}$ defines the metric for the matrix principal components analysis which renders it equivalent to the functional principal components analysis defined by equation (14). An alternative expression for equation (20) is

$$\mathbf{N}^{1/2}\mathbf{V}\mathbf{N}^{1/2}\mathbf{v} = \mu\mathbf{v} \tag{21}$$

where $\mathbf{v}'\mathbf{v} = 1$ and $\mathbf{u} = \mathbf{N}^{-1/2}\mathbf{v}$, inverses being taken in the Moore–Penrose sense if $\mathbf{N}$ is singular. The vector $\mathbf{x}$ of values of the harmonic ξ are then recovered by

$$\mathbf{x} = \mathbf{K}\{\mathbf{f}(\mathbf{f}'\mathbf{f})^{-1}\mathbf{f}' + \mathbf{K}\}^{-1}\mathbf{u}. \tag{22}$$

References

Ansley, C. F., Kohn, R. and Wong, C.-M. (1993) Nonparametric spline regression with prior information. *Biometrika*, **80**, 75–88.

Besse, P. and Ramsay, J. O. (1986) Principal components analysis of sampled functions. *Psychometrika*, **51**, 285–311.

Crow, E. L. and Shimizu, K. (1988) *Lognormal Distributions: Theory and Applications*. New York: Dekker.

Dalzell, C. and Ramsay, J. O. (1993) Computing reproducing kernels with arbitrary boundary constraints. *SIAM J. Sci. Comput.*, **14**, 511–518.

Feldman, A. G. (1986) Once more on the equilibrium point hypotheses (L model) of motor control. *J. Motor Behav.*, **18**, 17–54.

Green, P. J. and Silverman, B. W. (1994) *Nonparametric Regression and Generalized Linear Models: a Roughness Penalty Approach*. London: Chapman and Hall.

Plamondon, R. (1991) On the origin of asymmetric bell-shaped velocity profiles. In *Tutorials in Motor Neuroscience* (eds J. Requin and G. E. Stelmach). Dordrecht: Kluwer.

——— (1992) A theory of rapid movements. In *Tutorials in Motor Behavior II* (eds G. E. Stelmach and J. Requin), pp. 55–69. New York: Elsevier.

Ramsay, J. O. (1982) When the data are functions. *Psychometrika*, **47**, 379–396.

Ramsay, J. O. and Dalzell, C. J. (1991) Some tools for functional data analysis (with discussion). *J. R. Statist. Soc.* B, **53**, 539–572.

Rice, J. A. and Silverman, B. W. (1991) Estimating the mean and covariance structure nonparametrically when the data are curves. *J. R. Statist. Soc.* B, **53**, 233–243.

Rothwell, J. C. (1987) *Control of Human Voluntary Movement*. London: Croom Helm.

Stoer, J. and Bulirsch, R. (1980) *Introduction to Numerical Analysis*. New York: Springer.

Ulrich, R. and Miller, J. (1993) Information processing models generating lognormally distributed reaction times. *J. Math. Psychol.*, **37**, 513–525.

Ulrich, R. and Wing, A. W. (1991) A recruitment theory of force–time relations in the production of brief force pulses: the parallel force unit model. *Psychol. Rev.*, **98**, 268–294.

Wahba, G. (1990) *Spline Models for Observational Data*. Philadelphia: Society for Industrial and Applied Mathematics.